HHS Public Access

Author manuscript

Biol Cell. Author manuscript; available in PMC 2021 May 11.

Published in final edited form as:

Biol Cell. 2020 November ; 112(11): 349–367. doi:10.1111/boc.202000058.

Plasma membrane to vacuole traffic induced by glucose starvation requires Gga2 dependent sorting at the trans-Golgi network

Destiney Buelto[*,1,3], **Chao-wei Hung**[*,1,2,4], **Quyen L. Aoh**[2,5], **Sagar Lahiri**[1], **Mara C. Duncan**[1]

[1]Department of Cell and Developmental Biology, University of Michigan

[2]Department of Biology, University of North Carolina at Chapel Hill

[3]Curriculum in Genetics and Molecular Biology, University of North Carolina at Chapel Hill

[4]Current address: Department of Medicine, University of California, San Diego

[5]Current address: Department of Biology, Gannon University

Abstract

Background Information—In the yeast Saccharomyces cerevisiae, acute glucose starvation induces rapid endocytosis followed by vacuolar degradation of many plasma membrane proteins. This process is essential for cell viability, but the regulatory mechanisms that control it remain poorly understood. Under normal growth conditions, a major regulatory decision for endocytic cargo occurs at the trans-Golgi network (TGN) where proteins can recycle back to the plasma membrane or can be recognized by TGN-localised clathrin adaptors that direct them towards the vacuole. However, glucose starvation reduces recycling and alters the localization and post-translational modification of TGN-localised clathrin adaptors. This raises the possibility that during glucose starvation endocytosed proteins are routed to the vacuole by a novel mechanism that bypasses the TGN or does not require TGN-localised clathrin adaptors.

Results—Here, we investigate the role of TGN-localised clathrin adaptors in the traffic of several amino acid permeases, including Can1, during glucose starvation. We find that Can1 transits through the TGN after endocytosis in both starved and normal conditions. Can1 and other amino acid permeases require TGN-localised clathrin adaptors for maximal delivery to the vacuole. Furthermore, these permeases are actively sorted to the vacuole, because ectopically forced de-ubiquitination at the TGN results in the recycling of the Tat1 permease in starved cells. Finally, we report that the Mup1 permease requires the clathrin adaptor Gga2 for vacuolar delivery. In contrast, the clathrin adaptor protein complex AP-1 plays a minor role, potentially in retaining permeases in the TGN, but it is otherwise dispensable for vacuolar delivery.

Conclusions and significance—This work elucidates one membrane trafficking pathway needed for yeast to respond to acute glucose starvation. It also reveals the functions of TGN localised clathrin adaptors in this process. Our results indicate that the same machinery is needed

Send correspondence to Mara C. Duncan phone: +1 734 763 4106 fax: +1 734 763 1166 mcduncan@umich.edu.

*these authors contributed equally

Author contributions: MCD conceptualized the study, performed experiments and data analysis, and wrote the manuscript. DB, CWH, and, QLA conceptualized the study, performed experiments and data analysis. SL performed experiments.

for vacuolar protein sorting at the GN in glucose starved cells as is needed in the presence of glucose. In addition, our findings provide further support for the model that the TGN is a transit point for many endocytosed proteins, and that Gga2 and AP-1 function in distinct pathways at the TGN.

Keywords

Vesicle trafficking; Clathrin; Endosomes; Endocytosis/exocytosis; Yeast

Introduction:

Glucose is the preferred energy source for many cells. In yeast, it activates signaling pathways that force the cells to engage in aerobic glycolysis (Broach, 2012). Under these conditions, acute glucose starvation causes nearly immediate changes in ATP levels, the cytosolic pH, and in signal transduction cascades (Dechant et al., 2010; Wilson et al., 1996). These changes regulate diverse aspects of cellular physiology. One effect of these changes is a massive change in the net flux of plasma membrane proteins to the vacuole (Lang et al., 2014). In the vacuole, these proteins are degraded. This process contributes to the survival mechanism during glucose starvation. This trafficking and subsequent degradative response is likely caused by both an elevation in the endocytosis of plasma membrane proteins and a reduction in their recycling back to the plasma membrane. However, the regulatory mechanisms responsible for this critical degradative response are not fully clear (Appadurai et al., 2020; Lang et al., 2014; Xu and Bretscher, 2014).

Several lines of evidence suggest that the trafficking pathways and regulatory mechanisms that control sorting to the vacuole induced by glucose starvation might differ from those involved in sorting to the vacuole in the presence of glucose. In the presence of glucose, some, if not all, endocytosed material transits through the *trans*-Golgi Network (TGN) (Becuwe and Leon, 2014; Day et al., 2018; Gournas et al., 2017). When endocytosed proteins arrive at the TGN, they can either be recycled to the plasma membrane or routed towards the vacuole via clathrin adaptor proteins that localize to the TGN. However, these clathrin adaptor proteins are also strongly affected by glucose starvation: they delocalize immediately in response to the dramatic reduction in ATP levels due to glucose starvation, and exhibit changes in post-translational modifications that may alter their functions (Aoh et al., 2011; Aoh et al., 2013). In addition, lipid phosphatase proteins that downregulate clathrin adaptor function also redistribute to the TGN specifically during glucose starvation (Faulhammer et al., 2007). These observations bring into question whether the clathrin adaptors at the TGN sort the proteins destined for vacuolar degradation in glucose starved cells. Indeed, vacuolar protein sorting at the TGN may be unnecessary in glucose starved cells because glucose starvation also impairs secretory traffic (Xu and Bretscher, 2014). In the absence of secretory traffic, which mediates recycling from the TGN, all endocytosed material could transit via default to the vacuole with no need for active sorting. In this scenario, glucose starvation induced degradative traffic would be fundamentally different from that induced by protein specific degradation cues in terms of requirements for TGN-localized clathrin adaptors, the role of ubiquitination at the TGN, and potential for recycling from the TGN. Here we explore this possibility.

Results:

Can1 transits through the TGN enroute to the vacuole in the presence of glucose

Several lines of evidence suggest that plasma membrane proteins destined for degradation under normal growth conditions transit through the TGN. In imaging studies, some plasma membrane transporters can be seen transiting through the TGN after endocytosis (Becuwe and Leon, 2014; Day et al., 2018; Gournas et al., 2017). Moreover, TGN-localized clathrin adaptors are required for the degradation of many endocytosed proteins, suggesting they play a role in vacuolar protein sorting of endocytosed (Becuwe and Leon, 2014; Deng et al., 2009; Scott et al., 2004; Stringer and Piper, 2011). We first verified the role of the TGN, and the importance of the TGN localized clathrin adaptors for degradation of plasma membrane proteins in the presence of glucose by testing whether endocytosed proteins transit through the TGN. To do this, we monitored the arginine transporter Can1, which in the absence of its substrate arginine, is highly enriched at the plasma membrane. When arginine is added to the growth media, Can1 is endocytosed and degraded in the vacuole (Ghaddar et al., 2014; Lang et al., 2014). Under steady state growth conditions, Can1-GFP accumulates at the plasma membrane, occasional puncta of Can1 are observed, likely reflecting Can1 undergoing biosynthetic traffic to the plasma membrane and/or basal levels of endocytosis and recycling, and vacuole fluorescence is low. After the addition of arginine, fluorescently tagged Can1 first accumulates in punctate structures followed by delivery to the vacuole as previously described (Gournas et al., 2017). This delivery continues for several hours in the presence of arginine, leading to increased vacuolar fluorescence over the course of hours. When compared to untreated cells, both the average number of Can1 puncta per cell and the average number of puncta that co-localize with Sec7 increased after 1hr of continued arginine treatment (Figure 1A). We also monitored this co-localization using time-lapse microscopy. We found many instances (35%) where pre-existing Sec7 compartments acquired Can1 signal (Figure 1B). For these experiments, we used cells heterozygous for Sec7-mcherry to mitigate potential deleterious effects the Sec7-mcherry fusion. Because the Can1 punctate structures are diffraction limited or near diffraction limited, we could use epi-fluorescence microscopy to monitor Can1 co-localization with markers of the TGN, which also localize to diffraction limited or near diffraction limited puncta. As an alternative test, we performed a similar experiment using the TGN localized clathrin adaptor Ent5 to label the TGN and imaged cells 15 minutes after continued arginine treatment. Although there were fewer overall Can1 puncta, many of them (>40%), were Ent5 positive during several frames of the imaged period (Figure 1C). These results indicate that Can1 transits through the TGN or an organelle closely associated with the TGN after continued arginine treatment.

To determine if Can1 transits through the TGN rather than an organelle adjacent to the TGN, we acutely inhibited cargo exit from the TGN using the lactone antibiotic Brefeldin A. In yeast cells lacking Egr6, which allows Brefeldin A to enter cells, Brefeldin A suppresses traffic in the early secretory system and clathrin dependent traffic at the TGN and endosomes by inhibiting a subset of Arf1 functions that are important for the formation of vesicles at the ER, Golgi, and TGN (Donaldson et al., 1992; Peyroche et al., 1999). We treated cells with Brefeldin A at the same time that we added arginine and monitored the localization of Can1-GFP after 40 minutes of continued arginine treatment. In control cells

treated with DMSO, Can1-GFP appeared in the vacuole after 40 minutes of continued arginine treatment in nearly every cell (Figure 2A). In contrast, when the cells were treated with Brefeldin A, the appearance of Can1-GFP in the vacuole was almost completely absent at this time. Instead, Can1-GFP localized to internal punctate structures and the plasma membrane in most cells. To describe this behavior quantitatively, we classified cells into three categories. Cells with primarily plasma membrane localization Can1-GFP were categorized as displaying 'plasma membrane' localization. Cells with three or more bright puncta with or without vacuolar localization of Can1-GFP were categorized as displaying 'punctate' localization. Cells with prominent vacuolar localization and two or fewer puncta were categorized as displaying 'vacuole' localization. Using this classification, most of the DMSO and arginine treated cells were classified as having vacuolar localization of Can1, whereas most of the Brefeldin A and arginine treated cells were classified as having punctate localization of Can1. To examine the identity of the punctate structures, we examined the co-localization of Can1 with the TGN localized clathrin adaptor Gga2 as a marker of the TGN (Daboussi et al., 2012). Slightly more than 20% of Can1 puncta also labeled Gga2 suggesting that some Can1 transits to the TGN or an organelle that fuses with the TGN in the presence of Brefeldin A (Figure 2B). To determine if the Can1 in internal puncta derived from endocytosis, we inhibited endocytosis with actin sequestering drug Latrunculin A, which block all forms of endocytosis in yeast (Ayscough et al., 1997; Prosser et al., 2011). We found that the punctate population of Can1 was completely abolished when cells were treated with Latrunculin A prior to arginine and Brefeldin A treatment (Figure 2B). This suggests that cargo in the puncta comes from the plasma membrane rather than biosynthetic delivery, consistent with prior reports that newly-synthesized transporters do not accumulate strongly in the TGN under normal conditions (Day et al., 2018; Martzoukou et al., 2018). Together these results indicate that after endocytosis, Can1 is sorted to TGN prior to delivery to the vacuole under normal growth conditions.

We next studied the role of clathrin adaptors in substrate induced degradation of Can1by monitoring its traffic to the vacuole in cells lacking pairs of TGN localized clathrin adaptors (*apl4Δgga2Δ, gga2Δent5Δ, ent3Δent5Δ)*. These mutant combinations disrupt clathrin dependent exit from the TGN (Costaguta et al., 2006; Costaguta et al., 2001; Duncan et al., 2003; Zhdankina et al., 2001). In wild-type cells, Can1-GFP signal was clearly apparent in the vacuole in ~40% of the cells one hour after continued arginine treatment (Figure 3A). In contrast, in the double mutants significantly fewer cells (<15%) displayed vacuolar signal at this time point. Instead, many cells showed Can1-GFP in punctate structures. However, by three hours of treatment, some vacuolar Can1-GFP localization was observed in double mutants (Figure 3A). This suggests that adaptor mediated vacuolar protein sorting is important for vacuolar delivery, but in its absence some Can1 can reach the vacuole via alternate routes as proposed by others or that the adaptor mutant pairs used here do not fully impair the pathway (Gournas et al., 2017). We made similar observations whether we imaged cells live or arrested traffic with metabolic toxins as described in the material and methods, which allowed quantification of the defect at different time points. Using the quantitative classifications, we found that the percentage of cells classified as vacuolar was significantly lower in the mutants compared to wild-type cells at one hour (Figure 3A), but that by three hours only *apl4Δgga2Δ* showed a statistically significant difference.

We also examined vacuolar delivery by monitoring the levels of Can1 by western blot in wild-type and mutant cells. In wild-type cells, Can1–3HA levels were reduced by 25% 30 minutes after continued arginine treatment. In contrast, in *apl4Δgga2* or *gga2Δent5Δ* cells this decrease did not occur and Can1 levels seemed to increase, likely due to continued synthesis (Figure 3B). This difference indicates that clathrin adaptors are important for substrate induced vacuolar protein sorting of Can1.

Clathrin adaptors at the TGN are important for vacuolar protein sorting during glucose starvation

We next asked whether, during glucose starvation, Can1 also transits through the TGN. After glucose starvation, fluorescently tagged Can1 first accumulates in punctate structures followed by delivery to the vacuole as previously described (Lang et al., 2014). At one hour after continued glucose starvation, we found that the average number of Can1-GFP puncta that co-localized with Sec7 increased compared to untreated cells, indicating that during glucose starvation at least some Can1 transits through the TGN (Figure 1A).

We next tested whether clathrin adaptors are also important for Can1 vacuolar sorting during glucose starvation using adaptor mutant cells. In WT cells, within one hour after continued glucose starvation, Can1-GFP localized to internal punctate structures and the vacuole in some cells (Figure 4A). Three hours after continued glucose starvation, nearly all wild-type cells exhibited strong vacuolar localization of Can1-GFP. In contrast to the wild-type cells, the double mutants displayed limited Can1-GFP delivery to the vacuole after glucose starvation. These differences were apparent 1 hour after glucose starvation for the mutant combinations *apl4Δ gga2Δ* and *ent5Δ gga2Δ*. At this point, these mutant combinations had fewer cells with vacuolar Can1-GFP localization, and more with punctate Can1-GFP localization than wild-type cells. The differences became more striking three hours after continued glucose starvation. In wild-type cells, nearly every cell exhibited vacuolar localization of Can1-GFP. In contrast, in all three mutant combinations, fewer than 50% of cells showed vacuolar localization. We also monitored vacuolar delivery by monitoring the levels of Can1 by western blot in wild-type and mutant cells. Can1–3HA protein levels were reduced by ~50% in wild-type cells after 4 hours of glucose starvation (Figure 4B). Under these conditions, Can1 was significantly stabilized in *apl4Δ gga2Δ* cells, which exhibited the strongest effect. These data indicate clathrin adaptors are important for efficient degradative traffic of Can1-GFP in response to glucose starvation.

We next asked whether other plasma membrane proteins also depend on adaptors for traffic to the vacuole during glucose starvation. We tested several additional amino acid transporters that are known to be delivered to the vacuole in response to glucose starvation. We found that the delivery of Mup1, Tat2, and Tat1 were impaired in *apl4Δ gga2Δ* cells, suggesting that adaptor mediated vacuolar protein sorting at the TGN is likely a common requirement for the degradation of many transporters during glucose starvation (Figure 5A, B, and Figure 7).

Adaptors re-localize to the cytosol only transiently after glucose starvation

The finding that adaptors are important for vacuolar protein sorting during glucose starvation is unexpected because adaptor functions are sensitive to glucose starvation (Aoh et al., 2011). Immediately after glucose starvation, adaptors rapidly disassociate from the TGN. However, as the cells adapt to starvation, adaptors re-localize to the TGN. This raises the possibility that adaptors re-localize early enough after starvation to participate in vacuolar protein sorting.

To determine whether adaptors return to the TGN while in a time-frame consistent with a role in vacuolar protein sorting during glucose starvation, we monitored the localization of Ent5, Gga2, and AP-1 at 5, 15, and 120 minutes of continued glucose starvation. All three adaptors showed more punctate localization at 15 minutes than at 5 minutes, suggesting they begin to re-localize shortly after the onset of glucose starvation (Figure 6A). To better understand the kinetics of this recovery, we monitored Ent5-GFP with time-lapse microscopy. Immediately after glucose starvation, Ent5 was absent from the TGN, labeled by Sec7. However, upon continued starvation, Ent5 became visible co-localizing with Sec7 at about 8 minutes (Figure 6B). Similar kinetics were observed for Gga2 (Figure 6C). This suggests that the delocalization of clathrin adaptors is highly transient, and that adaptors re-localize to the TGN in a time-frame consistent with their role in degradative traffic.

Recycling pathways are active during glucose starvation

Finally, we analyzed whether the plasma membrane proteins cargo destined for vacuolar degradation are actively sorted at the TGN during glucose starvation. Under normal growth conditions, clathrin adaptors both recognize the cargo to be transported and assembling the clathrin coat that mediates traffic. It is thought that without active recognition of the cargo by adaptors, endocytosed proteins recycle back to the plasma membrane (Becuwe and Leon, 2014; Gournas et al., 2017). However, we previously reported that recycling rates of bulk membranes are strongly reduced by glucose starvation, thus all endocytosed cargo may be delivered to the vacuole by default (Lang et al., 2014). If recycling is strongly impaired during glucose starvation, active sorting would be unnecessary and adaptors would only be required to maintain the trafficking route, not cargo recognition. To explore whether active sorting occurs at the TGN during glucose starvation, we used a strategy that has previously be used to induce recycling from the TGN (Stringer and Piper, 2011). This strategy relies on the fusion of the viral de-ubiquitinase UL36 to Gga2. In prior work, this fusion protein prevents the vacuolar delivery of several transporters under conditions where they would normally be degraded. To test if recycling can occur from the TGN in glucose starved cells, we monitored re-localization of the tryptophan transporter Tat1-GFP. In cells expressing an empty vector control plasmid continued glucose starvation induced the vacuolar localization of Tat1-GFP in most cells (Figure 7). In contrast, in cells expressing Gga2-UL36, under the same conditions most cells had Tat1 localized at the plasma membrane after 2 hours of continued glucose starvation. Notably, the phenotype caused by Gga2-UL36 was different from that of the adaptor mutant for which most cells had Tat1 localized to puncta at 2 hours of glucose starvation (Figure 7). This suggests the effect of Gga2-UL36 is not a consequence of loss of adaptor function at the TGN. Finally, as a control for the specificity of this effect, we examined the effect of fusing UL36 to Hse1, a protein involved in multi-vesicular body

formation. In cells expressing Hse1-UL36, Tat1-GFP was predominantly on internal compartments, either puncta or the vacuole membrane at 2 hours after continued glucose starvation. This is similar to observations previously made for substrate induced degradation, and suggests that the plasma membrane localization seen in Gga2-UL36 expressing cells is specific to the Gga2-fusion (Stringer and Piper, 2011). Together these results indicate that recycling can occur even during glucose starvation.

Gga2 plays a major role in traffic from the TGN towards the vacuole in glucose starvation and substrate induced degradative traffic

Based on genetic interactions, the Gga proteins and AP-1 are thought to mediate different aspects of traffic at the TGN, however the exact role of each adaptor and their relationship to one another is unclear. Early studies looking at effects of deletion mutations on the kinetics of traffic to the vacuole, suggested that the Gga proteins and AP-1 may mediate parallel pathways from the TGN to the endosomes (Costaguta et al., 2001). This model suggests that to impair degradative traffic from the plasma membrane through the TGN and subsequently to the vacuole, both Gga and AP-1 pathways need to be disrupted. This model guided our selection of the pairs of TGN localized clathrin adaptors (*apl4Δgga2Δ, gga2Δent5Δ, ent3Δent5Δ)* used to block exit from the TGN. However, a more recent model suggests that for biosynthetic traffic, AP-1 may not function in traffic from the TGN to the endosomes, but rather functions exclusively in recycling within the TGN (Casler et al., 2019).

To determine whether the Gga proteins and AP-1 function in parallel pathways for post-endocytic vacuolar protein sorting, we compared the effect of single and double mutations on the vacuolar sorting of Mup1. Surprisingly, we found that deletion of *GGA2* alone impaired the vacuolar delivery of Mup1 in response to glucose starvation as strongly as deletion of both *GGA2* and *APL4*, whereas deletion of *APL4* had no detectable effect under these conditions (Figure 8). Similarly, cells lacking *GGA2* alone had as severe of an effect on the vacuolar delivery of Mup1 in response to its substrate methionine as did cells lacking both *GGA2* and *APL4*. Under these conditions, in most wild-type cells Mup1 was apparent in the vacuole 1hr after the addition of substrate, and little Mup1 was apparent at the cell surface. In contrast, in *gga2Δ* or *apl4Δgga2Δ* cells, only a small amount of Mup1 was delivered to the vacuole 1hr after the addition of substrate, and most cells had substantial Mup1 at the cell surface. To quantify this effect, we measured the intensity of the plasma membrane compared to the vacuole for individual cells, we used the ratio of this intensity to define cells as having high, medium, or low vacuolar intensity as described in the Casler et al., 2019. Using these criteria, less than 5% of wild-type cells had low intensity vacuoles and 50% had high intensity vacuoles one hour after the addition of methionine. In contrast, over 75% of *gga2Δ* or *apl4Δgga2Δ* cells had low intensity vacuoles and almost no cells had high intensity vacuoles under the same conditions. These data strongly argue that Gga2 plays the primary role in post-endocytic vacuolar protein sorting at the TGN during glucose starvation and in response to substrate.

Discussion:

Vacuolar protein sorting at the TGN remains intact during glucose starvation

Glucose starvation causes many cell surface proteins to be endocytosed, sorted to the vacuole, and then degraded (Lang et al., 2014). The molecular mechanisms guiding this large scale degradative response remain unclear. Notably, under normal growth conditions, endocytosis and subsequent vacuolar protein sorting is highly selective and requires regulatory scrutiny at several locations (Lauwers et al., 2010). A key location for this regulatory scrutiny is the TGN. At the TGN, clathrin adaptor proteins recognize proteins destined for degradation and sort them away from proteins destined to be secreted or recycled (Becuwe and Leon, 2014; Deng et al., 2009). However, during glucose starvation the clathrin adaptors are post-translationally modified, and their localization to the TGN is reduced (Aoh et al., 2011). In addition, recycling rates are reduced (Lang et al., 2014). This raises the possibility that the elevated degradative response during glucose starvation results from a reduction in the normal regulatory scrutiny at the TGN either by reducing the requirement for vacuolar protein sorting or reducing recycling or both. Our results indicate that despite these changes, the normal regulatory scrutiny at the TGN is intact during glucose starvation.

By several metrics, the requirements for vacuolar protein sorting remain intact during glucose starvation. First, cargo enters the TGN similar to its behavior during substrate induced degradative traffic. Moreover, clathrin adaptors are important for glucose starvation induced vacuolar protein sorting despite their reduced localization to the TGN and changes in post translational modifications. Notably, the effects of the double mutant combinations on vacuolar protein sorting appear similar in glucose starvation induced and substrate induced vacuolar protein sorting. Consistently, *apl4Δ gga2Δ* cells displayed stronger defects than *ent5Δ gga2Δ* cells, and *ent3Δ ent5Δ* cells showed the least defect whether substrate or glucose starvation was used as the degradative cue. This argues that the overall function of each adaptor is not dramatically altered by glucose starvation. Finally, although bulk membrane recycling rates as measured by FM4–64 are reduced during glucose starvation (Lang et al., 2014), we find that Gga2-UL36 can drive recycling of Tat1 from the TGN during glucose starvation. This indicates that during glucose starvation recycling of cargo proteins can still occur.

One remaining question is the role and regulation of ubiquitination in glucose starvation induced degradation. Although, based on our results, we cannot exclude the possibility that Gga2-UL36 and Hse1-UL36 act on the sorting machinery rather than the cargo, the finding that both Gga2-UL36 and Hse1-UL36 prevent the vacuolar delivery could imply that that glucose starvation stimulates the ubiquitination of plasma membrane proteins, and that this ubiquitination status is maintained at least until endocytosed proteins exit the TGN. In support of this model, a single ubiquitin on Mup1 causes constitutive degradation of Mup1 and bypasses the effect of both Gga2-UL36 and Hse1-UL36 suggesting that in the presence of glucose deubiquitination of cargo causes recycling (Stringer and Piper, 2011). Similarly, cargo ubiquitination has previously been established as contributing to the degradation of some glucose transporters in response to a shift from glucose to a non-fermentable carbon

source (Hovsepian et al., 2017). In this case the arrestin, Csr2/Art8 is required for degradation of Hxt2 and Hxt4 but not Hxt3 and Hxt1. The relevant arrestin(s), if any, which contribute to the glucose starvation induced degradation of the transporters studied here remain unknown. Finally, it remains to be determined whether dynamic cycles of de-ubiquitination and re-ubiquitination occur during glucose starvation similar to what has been suggested for other degradative cues (Becuwe and Leon, 2014; Gournas et al., 2017).

The TGN is a transit point for endocytic cargo during glucose starvation

This work also provides support for the emerging view that the TGN is a transit point for most, if not all endocytic cargo. We find that Can1 transits through the TGN both in the presence and absence of glucose, and that TGN localized clathrin adaptor are important for vacuolar protein sorting in response to glucose (Can1, Mup1, Tat1, and Tat2) and substrate (Can1, Mup1). These findings are consistent with prior reports about the loss of the Gga proteins or their co-factors on post-endocytic traffic to the vacuole of plasma membrane proteins such as Tat1, Ste3, Fur4, and Gap1 (Becuwe and Leon, 2014; Morvan et al., 2015; Scott et al., 2004; Sipos et al., 2004). The mechanistic explanation of these prior observations was initially unclear. Early models suggested Gga proteins acted in vacuolar proteins sorting at the multi-vesicular body (Deng et al., 2009; Eugster et al., 2004; Scott et al., 2004). However, later work revealed that Ggas co-localize with markers of the TGN such as Sec7 but not markers of the multi-vesicular body, challenging a direct role for Gga proteins in sorting at the multi-vesicular body (Daboussi et al., 2012; Day et al., 2018). More recently, live cell microscopy revealed endocytosed material including FM4–64 and Mup1 enter the TGN shortly after endocytosis, indicating the TGN is a component of the endocytic system (Day et al., 2018). This itinerary through the TGN was previously described for the post-endocytic traffic of the lactate transporter Jen1 (Becuwe and Leon, 2014). At the time, it was unclear whether this was an exceptional behavior of a unique cargo protein or a more common phenomenon. Our findings add additional evidence that transit through the TGN is a common behavior of several transporters under diverse degradative cues. It remains to be determined how many other cargos take this route, and if specific features of cargo dictate this itinerary.

The impact of Brefeldin A on endocytosis in yeast

Our finding that Brefeldin A impairs the traffic of endocytosed Can1 to the vacuole raises intriguing questions about the intersection of secretion and endocytosis. Although Brefeldin A is best known for its effects on secretion, effects on the delivery of FM4–64 and mating pheromone to the vacuole were previously described (Gaynor et al., 1998; Nagano et al., 2019). Moreover, mutations in both *ARF1* and *SEC7* cause defects in endocytosis suggesting Arf1 function at the TGN are important for endocytosis (Riezman, 1985; Yahara et al., 2001). Therefore, we interpret the defect in Can1 traffic caused by Brefeldin A to reflect an effect on clathrin adaptor mediated exit from the TGN. However, it is important to note that we cannot exclude that this endocytic defect is a secondary effect of the inhibition of secretion caused by Brefeldin A. Notably, early studies showed that many secretory mutations are defective in endocytosis, suggesting that impairing secretion could impair Can1 delivery to the vacuole (Hicke et al., 1997; Penalver et al., 1999; Riezman, 1985). One possible explanation for the involvement of ER to Golgi traffic comes from work showing

that secretory traffic controls the delivery of factors important for the formation of endocytic vesicles (Carroll et al., 2012; Johansen et al., 2016). In this case, Brefeldin A would inhibit endocytosis by preventing or slowing internalization. However, this mechanism is unlikely to explain the effect of Brefeldin A on Can1, because Can1 accumulated at intracellular compartments in cells treated with both Brefeldin A and arginine. An alternative model is that because the TGN matures from the Golgi, which itself matures from the transitional ER, in the absence of secretion, the TGN become non-functional for endocytic traffic (Pantazopoulou and Glick, 2019; Tojima et al., 2019). Indeed, the Golgi and TGN dissipate when some steps in the secretory pathway are blocked (Morin-Ganet et al., 2000; Papanikou et al., 2015). It will therefore be interesting to revisit the effect of secretory mutations on endocytosis given the growing appreciation of the role of the TGN in endocytosis.

Differential roles for clathrin adaptors at the TGN

In addition, this work provides evidence about the individual, distinct functions of the Gga and AP-1 pathways at the TGN. We found that the deletion of *GGA2* alone was nearly as defective as deletion of both *GGA2* and *APL4* for vacuolar protein sorting of Mup1 in response to either substrate or glucose starvation. This observation suggests that the Gga pathway plays a major role in vacuolar protein sorting Mup1 under both conditions. This role in vacuolar protein sorting is consistent with prior findings that show Gga proteins are required for sorting of other endocytosed plasma membrane proteins (Becuwe and Leon, 2014; Scott et al., 2004; Stringer and Piper, 2011). The strong effect of Gga2 on vacuolar protein sorting is notable because Gga2 is frequently considered to be functionally redundant with the closely related Gga1 protein. However, a large body of diverse evidence now indicates that Gga2 performs one or more unique functions. In diploid cells, Gga2 is important for genotoxic stress resistance and diploid cells lacking Gga2 exhibit high levels of genomic instability (Krol et al., 2015). Moreover, deletion of *GGA2* shows complete synthetic lethality with mutation of the arrestin *LDB19*, suggesting that Gga1 is unable to compensate for Gga2 for one or more critical functions (Martinez-Marquez and Duncan, 2018; Zhao et al., 2013). Although it remains to be determined the extent to which loss *GGA2* alone impairs the degradation of cell surface proteins, deletion of *GGA2* disrupts the vacuolar protein sorting of the siderophore transporters Sit1, and Arn1 suggesting that this may be a general effect (Deng et al., 2009; Erpapazoglou et al., 2008; Kim et al., 2007).

Although our results indicate AP-1 is dispensable for vacuolar protein sorting in the presence of Gga2, it is notable that in our analysis of the effect of double mutants on Can1 traffic, *apl4Δ gga2Δ* cells consistently displayed slightly stronger defects than *ent5Δ gga2Δ* cells. This observation suggests that although Gga2 is likely a major factor in vacuolar protein sorting, AP-1 performs some supplementary function. The observation that loss of AP-1 enhances the vacuolar protein sorting defect caused by Gga2 for endocytosed proteins enhancement is analogous to the effects AP-1 on vacuolar sorting of the vacuolar protease carboxypeptidase S in cells lacking Gga2 (Costaguta et al., 2001). As with Can1, deletion an AP-1 subunit gene does not impair carboxypeptidase S traffic on its own, however it enhances a carboxypeptidase S defect caused by deletion of *GGA2*. The mechanistic explanation for how loss of AP-1 enhances the defect caused by *GGA2* deletions is unclear. One possible explanation is that Ggas and AP-1 function in parallel vacuolar protein sorting

pathways, but that Mup1, and potentially the other transporters, exclusively transit via the Gga pathway. This model was originally proposed to explain the defects in CPS sorting (Costaguta et al., 2001). An alternate model is that AP-1 retains endocytosed proteins within the dynamically maturing TGN. In this case, in the absence of Gga2 the endocytosed transporters are retained in the TGN by AP-1. This retention allows limited delivery to the vacuole via an inefficient alternative route. When a defect in AP-1 is added, transporters recycle to the plasma membrane faster, thereby reducing the limited vacuolar traffic even further. Although a role for AP-1 in retaining proteins in the TGN is supported by previous studies, additional studies will be needed to completely clarify the role of AP-1 in this process (Casler et al., 2019; Foote and Nothwehr, 2006; Liu et al., 2008; Valdivia et al., 2002).

Finally, our results argue against a major role for AP-1 in the secretion of the transporters studied here. Several lines of evidence suggest AP-1 might participate in secretory traffic in other organisms. In epithelia of mammals, worms, and flies, AP-1 contributes to both apical and basolateral sorting, and in budding yeast an AP-1 binding partner is implicated in the formation of a subclass of secretory vesicles (Caceres et al., 2019; Castillon et al., 2018; Folsch, 2015; Gall et al., 2002; Gillard et al., 2015; Gravotta et al., 2019; Kametaka et al., 2012; Liu et al., 2008). Moreover, AP-1 appears to be important for secretory traffic in the filamentous yeast *Aspergillus nidulans*, therefore, it might be expected that in budding yeast AP-1 would participate in secretory traffic (Martzoukou et al., 2018). However, if AP-1 plays a role in secretion in budding yeast, its loss is not enough to cause accumulation of transporters in intracellular compartments in the absence of a degradative cue, either on its own or in combination with other adaptor mutants for the proteins investigated here.

In summary, despite the changes at the TGN that might suggest glucose starvation would induce a fundamentally different form of degradative traffic, we find no evidence for a novel degradative route induced by glucose starvation. We conclude that during glucose starvation, the endocytosed amino acid transporters examined here traffic through the TGN enroute to the vacuole, and are sorted by clathrin adaptors into this degradative route. Moreover, we report that for Mup1, at least, the adaptor Gga2 is the primary player in vacuolar protein sorting. Together these results provide additional support to the recent model that the TGN is a major sorting station for endocytosed proteins and suggest that this degradative route is common to many cell surface proteins responding to diverse degradative cues (Becuwe and Leon, 2014; Day et al., 2018; Gournas et al., 2017).

Materials and Methods:

Strains and Media

Yeast strains and plasmids are listed in Table 1 and Table 2 respectively (Aoh et al., 2013; Lin et al., 2008; Sikorski and Hieter, 1989). Fluorescent tags and gene deletions were introduced by standard one-step PCR-based methods (Hailey et al., 2002; Longtine et al., 1998). Strains containing multiple genomic modifications were generated using mating followed by tetrad dissections.

Media, Antibodies and Reagents

Yeast cells were grown in yeast/peptone media supplemented with 2% glucose or synthetic media as described previously described supplemented with 2% glucose and an amino acid mix consisting of histidine (2 mg/ml), leucine (3 mg/ml), lysine (3 mg/ml), tryptophan (2 mg/ml), adenine (2 mg/ml), uracil (2 mg/ml), methionine (1 mg/ml) at 100X (Lang et al., 2014), or amino acid drop-out mix lacking one or more nutrients to maintain plasmid selection. For experiments using Mup1, methionine was omitted. For experiments using Tat2, only histidine, leucine and lysine were added. Antibodies against HA were from Santa Cruz. Alexa-633 secondary antibodies were from Invitrogen (Carlsbad, CA). ADH1 antibody was from Sigma. For experiments with UL36, cells were treated with 0.1μM copper sulfate two hours prior to glucose starvation to induce the expression of UL36 fusion protein.

Imaging

For live cell imaging, a 4-ml yeast culture was grown to early log phase in synthetic media supplemented with 2% glucose and the appropriate amino acids. For glucose withdrawal, cells were washed twice into the appropriate media without glucose. For arginine induced endocytosis, cells were washed into media containing 120 μg/ml L-arginine. For methionine induced endocytosis, cells were washed into media containing 10 μg/ml L-methionine. For most experiments, cells were mounted on untreated coverslips and observed without or without metabolic inhibition. For Figures 3 and 4, cells were harvested, resuspended in 50 μls of 100 mM sodium fluoride/100 mM sodium azide stop mix and incubated on ice no longer than 30 minutes before imaging. For Figure 6B, cells were affixed to a glass bottom petri plate with concanavalin A. With the exception of Figure 2A and 6A, a Nikon Ti-E inverted microscope with a 1.4 NA, 100X, oil-immersion objective was used for fluorescence microscopy. For Figure 2A, a BX61, Olympus microscope was used. For figure 6A, cells were imaged exactly as described in Aoh et al.

For FM4–64 labeling of the vacuole, FM4–64 in DMSO was added to growing cells to a concentration of 20μg/ml. Cells were incubated for 10 minutes and excess FM4–64 was removed with fresh media, cells were incubated for an additional 20 minutes prior imaging or additional treatments.

To induce endocytosis, cells were washed three times with glucose starvation media or washed into media containing substrate. For experiments using Brefeldin A with no other drugs, Brefeldin A (Acros Organics) in DMSO or DMSO was added to a final concentration of 150μM and cells were imaged or treated with arginine immediately. For BrefeldinA and Latrunculin A experiments, Latrunculin A (Sigma) or DMSO was added to a final concentration of 95μM and cells were incubated for 5 minutes before adding Brefeldin A or DMSO and incubated for an additional 5 minutes before imaging or the addition of arginine.

Image analysis was performed in ImageJ. For co-localization analysis, puncta were manually selected independently in each channel and the percentage of GFP or YFP puncta overlapping with mCherry structures was calculated for a central plane. For time-lapse microscopy in Figure 1, images were taken for a total duration of 2 minutes. Can1 puncta

that co-localized with Sec7 or Ent5 for more than two frames were scored as positive. For determining vacuole and plasma membrane intensities, images were first background subtracted using a 50 pixel rolling ball radius then, maximum intensity measurements were collected from a 3-pixel-wide line drawn through a representative region of the plasma membrane, and the vacuole. The ratio of vacuole to plasma intensity was determined for each cell, cells with vacuole intensity less than two times higher than plasma membrane were classified as low intensity, those with intensities between two and five times that of the plasma membrane were classified as medium, and those with intensities more than five times higher were classified as high intensity. Statistical significance was determined using a two-tailed student's t-test.

Whole-Cell Yeast Extracts

To generate lysates, 10 mls of log phase cells (0.2 OD_{600}) were pelleted, resuspended and incubated in 200 mM NaOH and precipitated by the addition of 0.1% trichloroacetic acid. TCA precipitates were disrupted by glass-bead mechanical disruption, pelleted, then washed in ice-cold acetone. TCA pellets were then resuspended in Laemmli sample buffer including urea and incubated at 37C for 5 minutes as previously described (Knop et al., 1999). Lysates were centrifuged at 13,000 rpm for 1 min and supernatants were used for immuno-blot analysis. Immuno-blots were blocked with 5% milk in TBS-T, and then probed with primary and fluorescent secondary antibodies. Fluorescence signals were detected on a Typhoon imaging system (Amersham). Protein intensities were quantitated by ImageJ.

Acknowledgements:

We thank Ajit Joglekar and Edward Salmon for use of and help with microscopy facilities and analysis. We thank Scott Emr, Robert Piper, and Amy Chang for generously sharing reagents. We also thank two anonymous reviewers and the editor for helpful comments that improved this work.

Funding: This work was supported by the National Institutes of Health [GM092741, GM129255] and funds from the Protein Folding Disease Initiative at the University of Michigan.

Abbreviations:

TGN	*trans*-Golgi Network

References

Aoh QL, Graves LM, and Duncan MC (2011). Glucose regulates clathrin adaptors at the trans-Golgi network and endosomes. Mol Biol Cell 22, 3671–3683. [PubMed: 21832155]

Aoh QL, Hung CW, and Duncan MC (2013). Energy metabolism regulates clathrin adaptors at the trans-Golgi network and endosomes. Mol Biol Cell 24, 832–847. [PubMed: 23345590]

Appadurai D, Gay L, Moharir A, Lang MJ, Duncan MC, Schmidt O, Teis D, Vu TN, Silva M, Jorgensen EM, et al. (2020). Plasma membrane tension regulates eisosome structure and function. Mol Biol Cell 31, 287–303. [PubMed: 31851579]

Ayscough KR, Stryker J, Pokala N, Sanders M, Crews P, and Drubin DG (1997). High rates of actin filament turnover in budding yeast and roles for actin in establishment and maintenance of cell polarity revealed using the actin inhibitor latrunculin-A. J Cell Biol 137, 399–416. [PubMed: 9128251]

Becuwe M, and Leon S (2014). Integrated control of transporter endocytosis and recycling by the arrestin-related protein Rod1 and the ubiquitin ligase Rsp5. eLife 3.

Broach JR (2012). Nutritional control of growth and development in yeast. Genetics 192, 73–105. [PubMed: 22964838]

Caceres PS, Gravotta D, Zager PJ, Dephoure N, and Rodriguez-Boulan E (2019). Quantitative proteomics of MDCK cells identify unrecognized roles of clathrin adaptor AP-1 in polarized distribution of surface proteins. Proc Natl Acad Sci U S A 116, 11796–11805. [PubMed: 31142645]

Carroll SY, Stimpson HE, Weinberg J, Toret CP, Sun Y, and Drubin DG (2012). Analysis of yeast endocytic site formation and maturation through a regulatory transition point. Mol Biol Cell 23, 657–668. [PubMed: 22190733]

Casler JC, Papanikou E, Barrero JJ, and Glick BS (2019). Maturation-driven transport and AP-1-dependent recycling of a secretory cargo in the Golgi. J Cell Biol 218, 1582–1601. [PubMed: 30858194]

Castillon GA, Burriat-Couleru P, Abegg D, Criado Santos N, and Watanabe R (2018). Clathrin and AP1 are required for apical sorting of glycosyl phosphatidyl inositol-anchored proteins in biosynthetic and recycling routes in Madin-Darby canine kidney cells. Traffic 19, 215–228. [PubMed: 29352747]

Costaguta G, Duncan MC, Fernandez GE, Huang GH, and Payne GS (2006). Distinct roles for TGN/endosome epsin-like adaptors Ent3p and Ent5p. Mol Biol Cell 17, 3907–3920. [PubMed: 16790491]

Costaguta G, Stefan CJ, Bensen ES, Emr SD, and Payne GS (2001). Yeast Gga coat proteins function with clathrin in Golgi to endosome transport. Mol Biol Cell 12, 1885–1896. [PubMed: 11408593]

Daboussi L, Costaguta G, and Payne GS (2012). Phosphoinositide-mediated clathrin adaptor progression at the trans-Golgi network. Nature cell biology 14, 239–248. [PubMed: 22344030]

Day KJ, Casler JC, and Glick BS (2018). Budding Yeast Has a Minimal Endomembrane System. Dev Cell 44, 56–72 e54. [PubMed: 29316441]

Dechant R, Binda M, Lee SS, Pelet S, Winderickx J, and Peter M (2010). Cytosolic pH is a second messenger for glucose and regulates the PKA pathway through V-ATPase. EMBO J 29, 2515–2526. [PubMed: 20581803]

Deng Y, Guo Y, Watson H, Au WC, Shakoury-Elizeh M, Basrai MA, Bonifacino JS, and Philpott CC (2009). Gga2 mediates sequential ubiquitin-independent and ubiquitin-dependent steps in the trafficking of ARN1 from the trans-Golgi network to the vacuole. The Journal of biological chemistry 284, 23830–23841. [PubMed: 19574226]

Donaldson JG, Finazzi D, and Klausner RD (1992). Brefeldin A inhibits Golgi membrane-catalysed exchange of guanine nucleotide onto ARF protein. Nature 360, 350–352. [PubMed: 1448151]

Duncan MC, Costaguta G, and Payne GS (2003). Yeast epsin-related proteins required for Golgi-endosome traffic define a gamma-adaptin ear-binding motif. Nature cell biology 5, 77–81. [PubMed: 12483220]

Erpapazoglou Z, Froissard M, Nondier I, Lesuisse E, Haguenauer-Tsapis R, and Belgareh-Touze N (2008). Substrate- and ubiquitin-dependent trafficking of the yeast siderophore transporter Sit1. Traffic 9, 1372–1391. [PubMed: 18489705]

Eugster A, Pecheur EI, Michel F, Winsor B, Letourneur F, and Friant S (2004). Ent5p is required with Ent3p and Vps27p for ubiquitin-dependent protein sorting into the multivesicular body. Mol Biol Cell 15, 3031–3041. [PubMed: 15107463]

Faulhammer F, Kanjilal-Kolar S, Knodler A, Lo J, Lee Y, Konrad G, and Mayinger P (2007). Growth control of Golgi phosphoinositides by reciprocal localization of sac1 lipid phosphatase and pik1 4-kinase. Traffic 8, 1554–1567. [PubMed: 17908202]

Folsch H (2015). Role of the epithelial cell-specific clathrin adaptor complex AP-1B in cell polarity. Cell Logist 5, e1074331. [PubMed: 27057418]

Foote C, and Nothwehr SF (2006). The clathrin adaptor complex 1 directly binds to a sorting signal in Ste13p to reduce the rate of its trafficking to the late endosome of yeast. J Cell Biol 173, 615–626. [PubMed: 16702232]

Gall WE, Geething NC, Hua Z, Ingram MF, Liu K, Chen SI, and Graham TR (2002). Drs2p-dependent formation of exocytic clathrin-coated vesicles in vivo. Curr Biol 12, 1623–1627. [PubMed: 12372257]

Gaynor EC, Chen CY, Emr SD, and Graham TR (1998). ARF is required for maintenance of yeast Golgi and endosome structure and function. Mol Biol Cell 9, 653–670. [PubMed: 9487133]

Ghaddar K, Merhi A, Saliba E, Krammer EM, Prevost M, and Andre B (2014). Substrate-Induced Ubiquitylation and Endocytosis of Yeast Amino Acid Permeases. Mol Cell Biol 34, 4447–4463. [PubMed: 25266656]

Gillard G, Shafaq-Zadah M, Nicolle O, Damaj R, Pecreaux J, and Michaux G (2015). Control of E-cadherin apical localisation and morphogenesis by a SOAP-1/AP-1/clathrin pathway in C. elegans epidermal cells. Development 142, 1684–1694. [PubMed: 25858456]

Gournas C, Saliba E, Krammer EM, Barthelemy C, Prevost M, and Andre B (2017). Transition of yeast Can1 transporter to the inward-facing state unveils an alpha-arrestin target sequence promoting its ubiquitylation and endocytosis. Mol Biol Cell 28, 2819–2832. [PubMed: 28814503]

Gravotta D, Perez Bay A, Jonker CTH, Zager PJ, Benedicto I, Schreiner R, Caceres PS, and Rodriguez-Boulan E (2019). Clathrin and clathrin adaptor AP-1 control apical trafficking of megalin in the biosynthetic and recycling routes. Mol Biol Cell 30, 1716–1728. [PubMed: 31091172]

Hailey DW, Davis TN, and Muller EG (2002). Fluorescence resonance energy transfer using color variants of green fluorescent protein. Methods Enzymol 351, 34–49. [PubMed: 12073355]

Hicke L, Zanolari B, Pypaert M, Rohrer J, and Riezman H (1997). Transport through the yeast endocytic pathway occurs through morphologically distinct compartments and requires an active secretory pathway and Sec18p/N-ethylmaleimide-sensitive fusion protein. Mol Biol Cell 8, 13–31. [PubMed: 9017592]

Hovsepian J, Defenouillere Q, Albanese V, Vachova L, Garcia C, Palkova Z, and Leon S (2017). Multilevel regulation of an alpha-arrestin by glucose depletion controls hexose transporter endocytosis. J Cell Biol 216, 1811–1831. [PubMed: 28468835]

Johansen J, Alfaro G, and Beh CT (2016). Polarized Exocytosis Induces Compensatory Endocytosis by Sec4p-Regulated Cortical Actin Polymerization. PLoS Biol 14, e1002534. [PubMed: 27526190]

Kametaka S, Kametaka A, Yonekura S, Haruta M, Takenoshita S, Goto S, and Waguri S (2012). AP-1 clathrin adaptor and CG8538/Aftiphilin are involved in Notch signaling during eye development in Drosophila melanogaster. Journal of cell science 125, 634–648. [PubMed: 22389401]

Kim Y, Deng Y, and Philpott CC (2007). GGA2- and ubiquitin-dependent trafficking of Arn1, the ferrichrome transporter of Saccharomyces cerevisiae. Mol Biol Cell 18, 1790–1802. [PubMed: 17344478]

Knop M, Siegers K, Pereira G, Zachariae W, Winsor B, Nasmyth K, and Schiebel E (1999). Epitope tagging of yeast genes using a PCR-based strategy: more tags and improved practical routines. Yeast 15, 963–972. [PubMed: 10407276]

Krol K, Brozda I, Skoneczny M, Bretner M, and Skoneczna A (2015). A genomic screen revealing the importance of vesicular trafficking pathways in genome maintenance and protection against genotoxic stress in diploid Saccharomyces cerevisiae cells. PLoS One 10, e0120702. [PubMed: 25756177]

Lang MJ, Martinez-Marquez JY, Prosser DC, Ganser LR, Buelto D, Wendland B, and Duncan MC (2014). Glucose starvation inhibits autophagy via vacuolar hydrolysis and induces plasma membrane internalization by down-regulating recycling. The Journal of biological chemistry 289, 16736–16747. [PubMed: 24753258]

Lauwers E, Erpapazoglou Z, Haguenauer-Tsapis R, and Andre B (2010). The ubiquitin code of yeast permease trafficking. Trends Cell Biol 20, 196–204. [PubMed: 20138522]

Lin CH, MacGurn JA, Chu T, Stefan CJ, and Emr SD (2008). Arrestin-related ubiquitin-ligase adaptors regulate endocytosis and protein turnover at the cell surface. Cell 135, 714–725. [PubMed: 18976803]

Liu K, Surendhran K, Nothwehr SF, and Graham TR (2008). P4-ATPase requirement for AP-1/clathrin function in protein transport from the trans-Golgi network and early endosomes. Mol Biol Cell 19, 3526–3535. [PubMed: 18508916]

Longtine MS, McKenzie A 3rd, Demarini DJ, Shah NG, Wach A, Brachat A, Philippsen P, and Pringle JR (1998). Additional modules for versatile and economical PCR-based gene deletion and modification in Saccharomyces cerevisiae. Yeast 14, 953–961. [PubMed: 9717241]

Martinez-Marquez JY, and Duncan MC (2018). Investigation of Ldb19/Art1 localization and function at the late Golgi. PLoS One 13, e0206944. [PubMed: 30403748]

Martzoukou O, Diallinas G, and Amillis S (2018). Secretory Vesicle Polar Sorting, Endosome Recycling and Cytoskeleton Organization Require the AP-1 Complex in Aspergillus nidulans. Genetics 209, 1121–1138. [PubMed: 29925567]

Morin-Ganet MN, Rambourg A, Deitz SB, Franzusoff A, and Kepes F (2000). Morphogenesis and dynamics of the yeast Golgi apparatus. Traffic 1, 56–68. [PubMed: 11208060]

Morvan J, de Craene JO, Rinaldi B, Addis V, Misslin C, and Friant S (2015). Btn3 regulates the endosomal sorting function of the yeast Ent3 epsin, an adaptor for SNARE proteins. Journal of cell science 128, 706–716. [PubMed: 25512335]

Nagano M, Toshima JY, Siekhaus DE, and Toshima J (2019). Rab5-mediated endosome formation is regulated at the trans-Golgi network. Commun Biol 2, 419. [PubMed: 31754649]

Pantazopoulou A, and Glick BS (2019). A Kinetic View of Membrane Traffic Pathways Can Transcend the Classical View of Golgi Compartments. Front Cell Dev Biol 7, 153. [PubMed: 31448274]

Papanikou E, Day KJ, Austin J, and Glick BS (2015). COPI selectively drives maturation of the early Golgi. eLife 4.

Penalver E, Lucero P, Moreno E, and Lagunas R (1999). Clathrin and two components of the COPII complex, Sec23p and Sec24p, could be involved in endocytosis of the Saccharomyces cerevisiae maltose transporter. J Bacteriol 181, 2555–2563. [PubMed: 10198022]

Peyroche A, Antonny B, Robineau S, Acker J, Cherfils J, and Jackson CL (1999). Brefeldin A acts to stabilize an abortive ARF-GDP-Sec7 domain protein complex: involvement of specific residues of the Sec7 domain. Mol Cell 3, 275–285. [PubMed: 10198630]

Prosser DC, Drivas TG, Maldonado-Baez L, and Wendland B (2011). Existence of a novel clathrin-independent endocytic pathway in yeast that depends on Rho1 and formin. J Cell Biol 195, 657–671. [PubMed: 22065638]

Riezman H (1985). Endocytosis in yeast: several of the yeast secretory mutants are defective in endocytosis. Cell 40, 1001–1009. [PubMed: 3886157]

Scott PM, Bilodeau PS, Zhdankina O, Winistorfer SC, Hauglund MJ, Allaman MM, Kearney WR, Robertson AD, Boman AL, and Piper RC (2004). GGA proteins bind ubiquitin to facilitate sorting at the trans-Golgi network. Nature cell biology 6, 252–259. [PubMed: 15039776]

Sikorski RS, and Hieter P (1989). A system of shuttle vectors and yeast host strains designed for efficient manipulation of DNA in Saccharomyces cerevisiae. Genetics 122, 19–27. [PubMed: 2659436]

Sipos G, Brickner JH, Brace EJ, Chen L, Rambourg A, Kepes F, and Fuller RS (2004). Soi3p/Rav1p functions at the early endosome to regulate endocytic trafficking to the vacuole and localization of trans-Golgi network transmembrane proteins. Mol Biol Cell 15, 3196–3209. [PubMed: 15090613]

Stringer DK, and Piper RC (2011). A single ubiquitin is sufficient for cargo protein entry into MVBs in the absence of ESCRT ubiquitination. J Cell Biol 192, 229–242. [PubMed: 21242292]

Tojima T, Suda Y, Ishii M, Kurokawa K, and Nakano A (2019). Spatiotemporal dissection of the trans-Golgi network in budding yeast. Journal of cell science 132.

Valdivia RH, Baggott D, Chuang JS, and Schekman RW (2002). The yeast clathrin adaptor protein complex 1 is required for the efficient retention of a subset of late Golgi membrane proteins. Dev Cell 2, 283–294. [PubMed: 11879634]

Wilson WA, Hawley SA, and Hardie DG (1996). Glucose repression/derepression in budding yeast: SNF1 protein kinase is activated by phosphorylation under derepressing conditions, and this correlates with a high AMP:ATP ratio. Curr Biol 6, 1426–1434. [PubMed: 8939604]

Xu L, and Bretscher A (2014). Rapid glucose depletion immobilizes active myosin V on stabilized actin cables. Curr Biol 24, 2471–2479. [PubMed: 25308080]

Yahara N, Ueda T, Sato K, and Nakano A (2001). Multiple roles of Arf1 GTPase in the yeast exocytic and endocytic pathways. Mol Biol Cell 12, 221–238. [PubMed: 11160834]

Zhao Y, Macgurn JA, Liu M, and Emr S (2013). The ART-Rsp5 ubiquitin ligase network comprises a plasma membrane quality control system that protects yeast cells from proteotoxic stress. eLife 2, e00459. [PubMed: 23599894]

Zhdankina O, Strand NL, Redmond JM, and Boman AL (2001). Yeast GGA proteins interact with GTP-bound Arf and facilitate transport through the Golgi. Yeast 18, 1–18. [PubMed: 11124697]

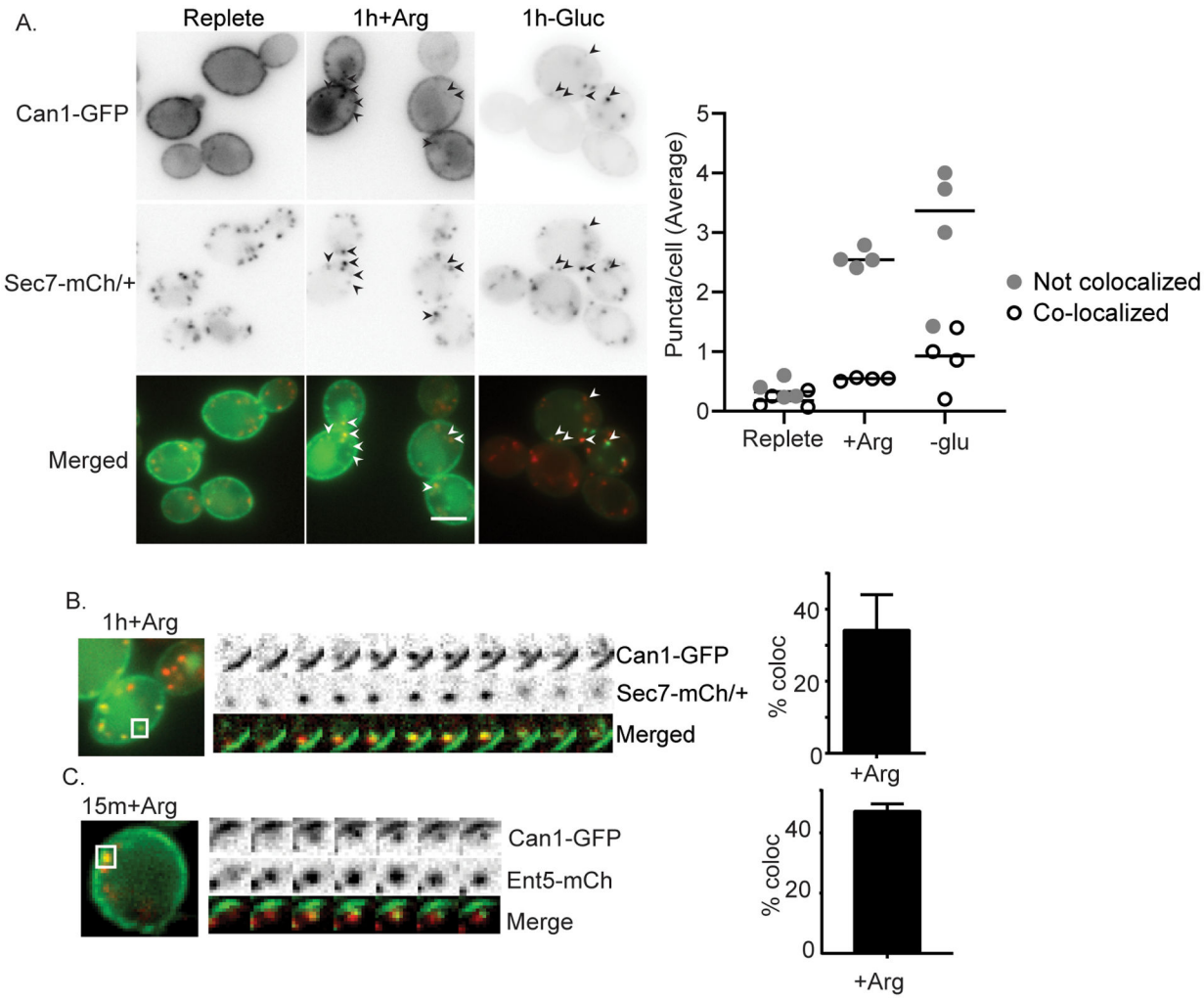

Figure 1.

Cargo co-localizes with markers of the TGN after substrate or glucose starvation induced endocytosis. A) Diploid cells heterozygous for Sec7-mCherry and expressing Can1-GFP from a plasmid were imaged under normal growth conditions (replete), or after continued arginine treatment, or continued glucose starvation. Arrowheads indicate co-localization. Co-localization was quantified as described in the materials and methods. Charts present average puncta per cell of each class from replicate experiments. B) Representative kymograph showing existing TGN structure acquiring Can1-GFP followed by dissipation of both signals with different kinetics. Each frame represents 2 seconds. Quantification of percent of Can-GFP structures that contained Can1-GFP and Sec7-mCherry for more than two frames was determined from movies. Charts show means with standard deviation, n=3. C) Representative kymograph showing Can1-GFP prolonged co-localization with Ent5-mCherry at early time points after continued arginine treatment. Imaging and quantification was performed as described for panel B.

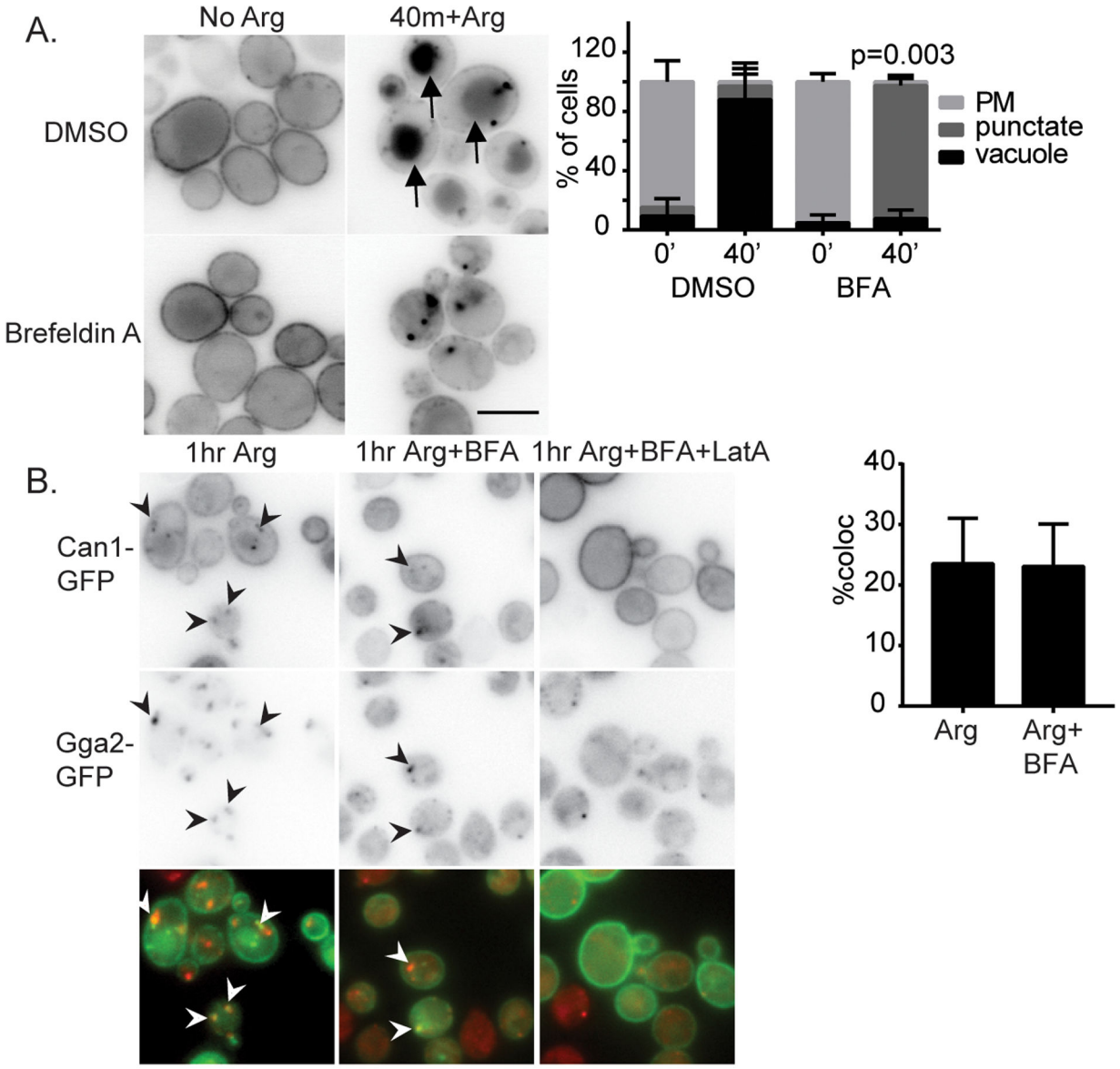

Figure 2.

Brefeldin A inhibits Can1 traffic to the vacuole in response to substrate. A) Cells lacking Erg6 and expressing Can1-GFP from a plasmid were grown in synthetic media and treated with DMSO as a vehicle control or 150 μM Brefeldin A and imaged immediately or 40 min after continued arginine treatment. Bar is 5 μm. Chart shows quantification of cell classes and p-values as described in materials and methods. B) Cells expressing Gga2-GFP from its endogenous locus and Can1-GFP from a plasmid were treated with indicated compounds and imaged after 1hr. Co-localization was quantified as described in the materials and methods. Charts show means with standard deviation, n=3. Latrunculin A treated cells had no puncta to quantify co-localization (n.d.).

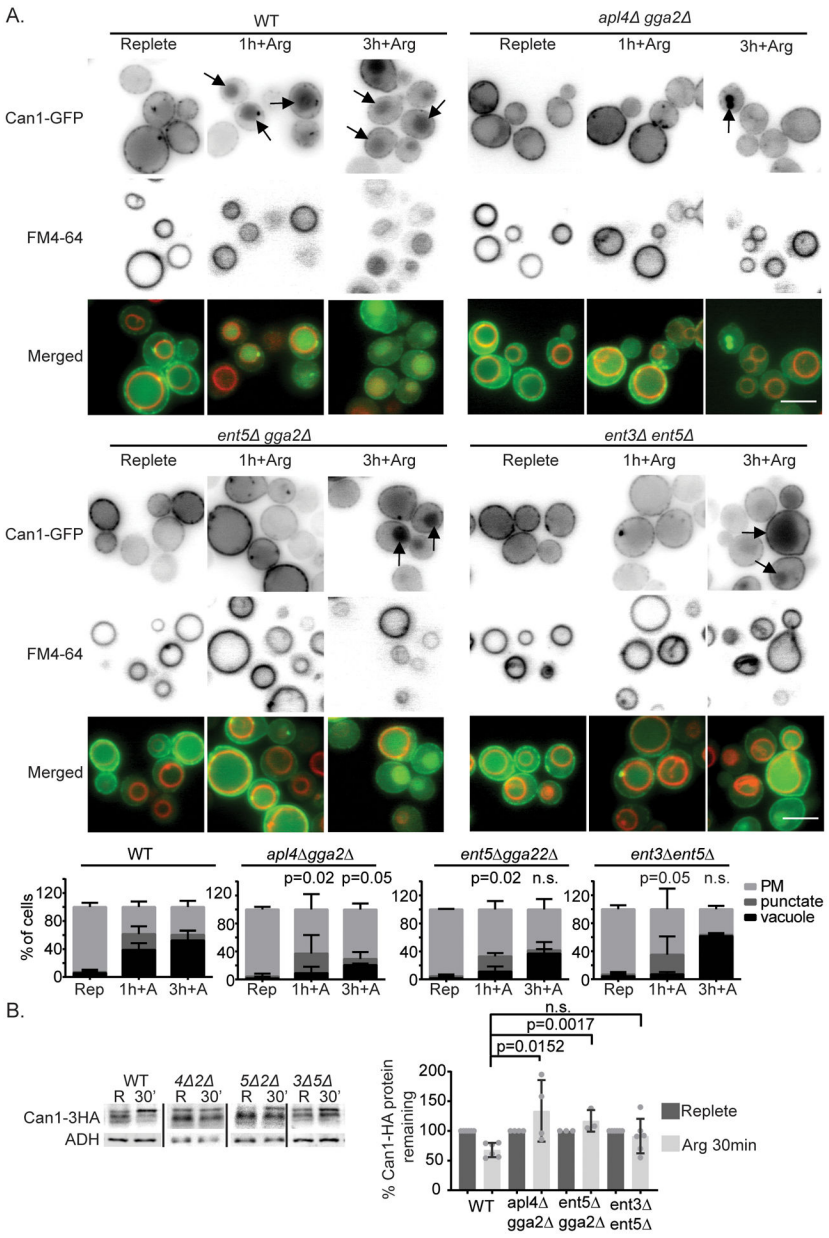

Figure 3.

TGN-localized clathrin adaptors are important for delivery of Can1 to the vacuole after arginine addition. A) Indicated cells expressing Can1-GFP from a plasmid were imaged in synthetic complete media and 1 or 3 hr after addition of 120mg/ml arginine. Arrows indicate vacuolar localization as identified by FM4–64 labeling. Bar is 5 μm. Chart shows quantification of cell classes and p-values as described in materials and methods, n=3. B) Can1-HA expressed from its endogenous locus was extracted from wild-type (WT), *apl4Δgga2Δ (4Δ2Δ), ent5Δ gga2Δ (5Δ2Δ),* or *ent3Δ ent5Δ (3Δ5Δ)* in replete media (R) and 30min after continued arginine treatment (30'). Image shows representative western blot probed for Can1-HA and lysis control ADH1. Charts show quantification of percent Can1-HA protein remaining at 30min after continued arginine treatment, means with standard

deviation are displayed, individual values are plotted. Values were normalized to Can1-HA before glucose withdrawal and lysis control ADH1. p-values were calculated using a two-tailed unpaired t-test for the null hypothesis that the average value was equal for mutant and wild-type cells.

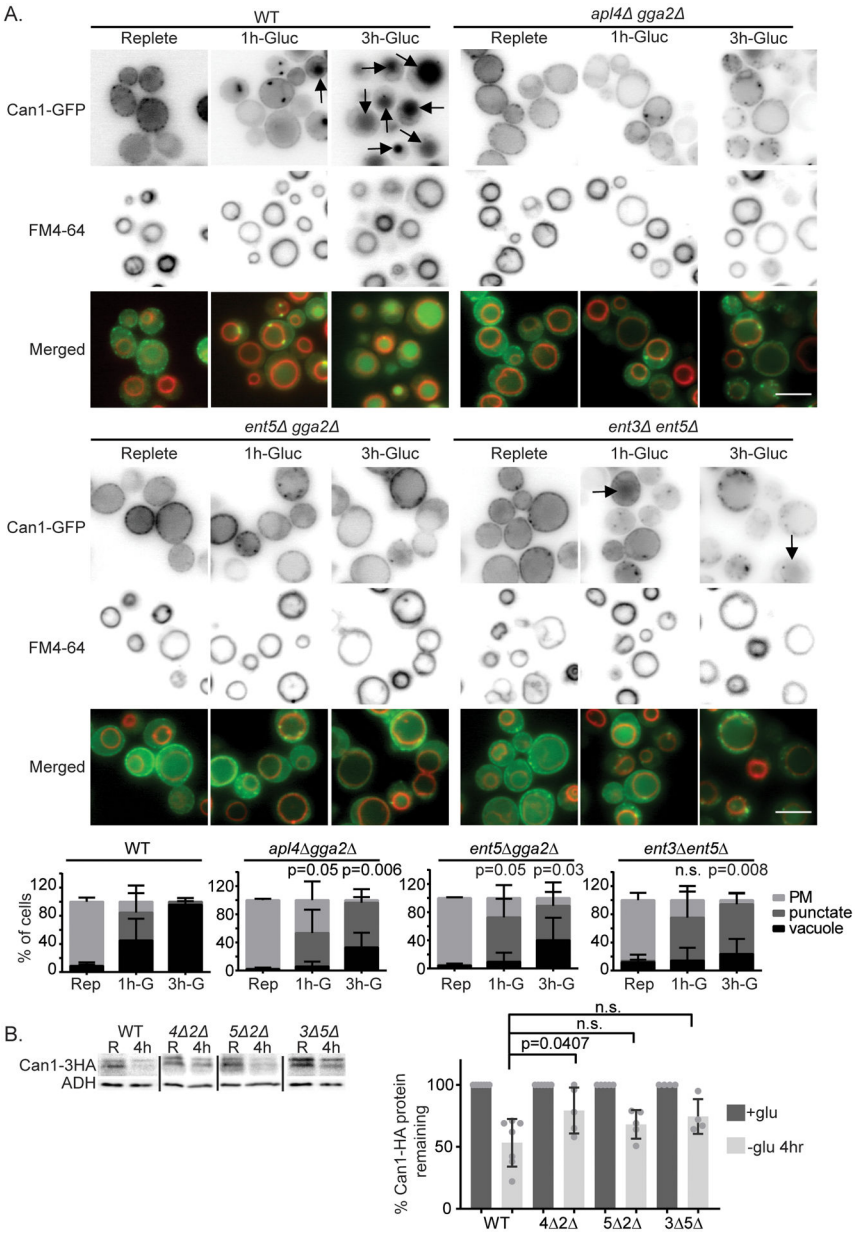

Figure 4.

TGN-localized clathrin adaptors are important for delivery of Can1 to the vacuole after glucose starvation. A) Indicated cells expressing Can1-GFP from a plasmid were imaged in synthetic complete media and 1 or 3 hr of continued glucose withdrawal. Arrows indicate vacuolar localization as identified by FM4–64 labeling. Bar is 5 μm. Chart shows quantification of cell classes and p-values as described in materials and methods, n=3. B) Can1-HA expressed from its endogenous locus was extracted from wild-type (WT), *apl4Δgga2Δ (4Δ2Δ), ent5Δ gga2Δ (5Δ2Δ),* or *ent3Δ ent5Δ (3Δ5Δ)* in replete media (R) and 4 hr after continued glucose withdrawal (30'). Image shows representative western blot probed for Can1-HA and lysis control ADH1. Charts show quantification of percent Can1-HA protein remaining at 30 min after continued arginine treatment, means with standard

deviation are displayed, individual values are plotted. Values were normalized to Can1-HA before glucose withdrawal and lysis control ADH1. p-values were calculated using a two-tailed unpaired t-test for the null hypothesis that the average value was equal for mutant and wild-type cells.

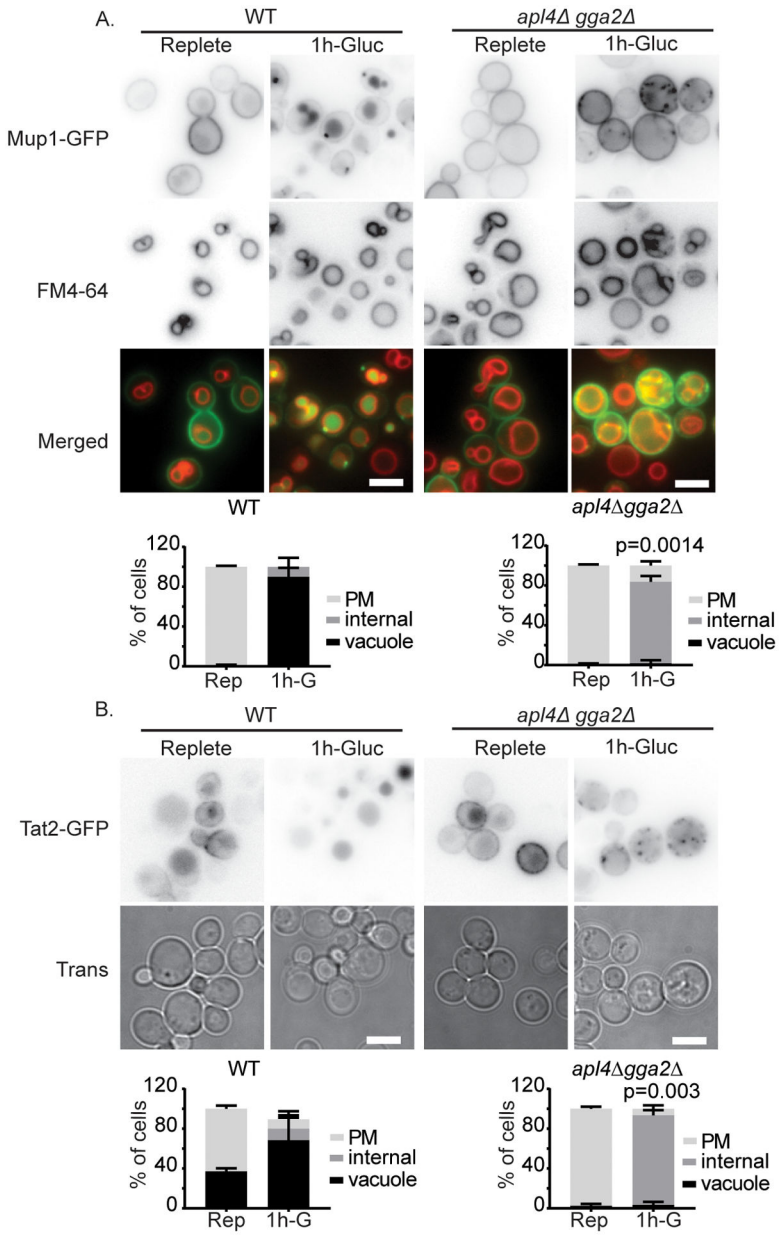

Figure 5.

TGN-localized clathrin adaptors are important for delivery of Mup1 and Tat2 to the vacuole after glucose starvation. A) Indicated cells expressing Mup1-GFP from a plasmid were imaged in synthetic complete media and 1 hr after continued glucose withdrawal. B) Indicated cells expressing Tat2-GFP from a plasmid were imaged in synthetic complete media and 1 hr after continued glucose withdrawal. Bars are 5 μm. Chart shows quantification of cell classes, p=values were calculated using a two-tailed unpaired t-test for the null hypothesis that the percentage of cells with vacuolar localization was equal for mutant and wild-type cells, means with standard deviation are displayed, n=3.

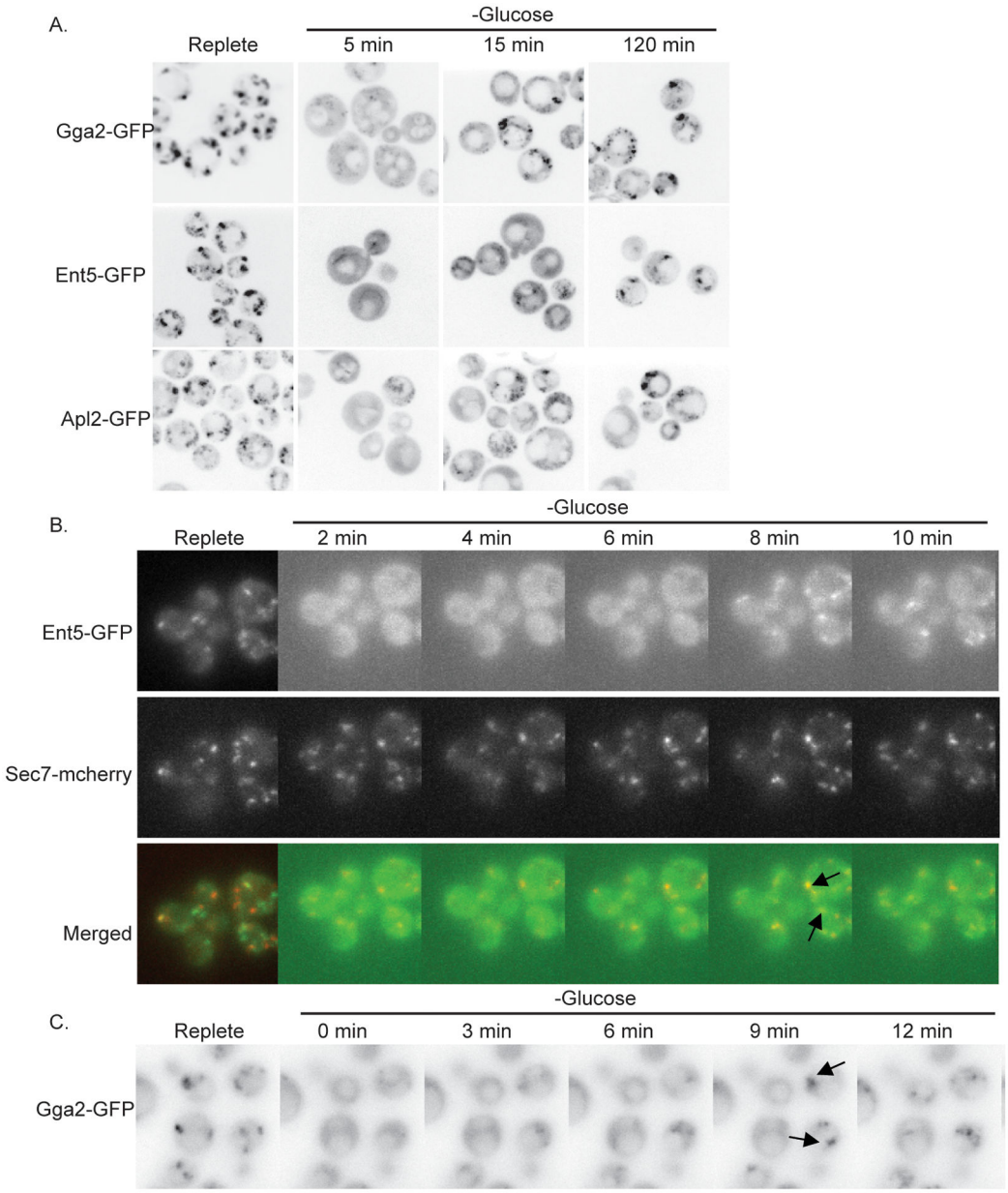

Figure 6.

Adaptors relocalize to the TGN within minutes of glucose starvation A) Wild-type cells expressing indicated fusion proteins from their endogenous loci were imaged under normal growth conditions (replete), or at indicated time points after continued glucose withdrawal. B) Wild-type cells expressing indicated fusion proteins from their endogenous loci were affixed to glass bottom dishes and imaged prior to and at indicated time points after continued glucose withdrawal. Arrows indicate Ent5 co-localization with Sec7-mcherry. C) Wild-type cells expressing Gga2-GFP from its endogenous locus were affixed to glass bottom dishes and imaged prior to and at indicated time points after continued glucose withdrawal. Arrows indicate recruitment of Gga2-GFP to intense foci.

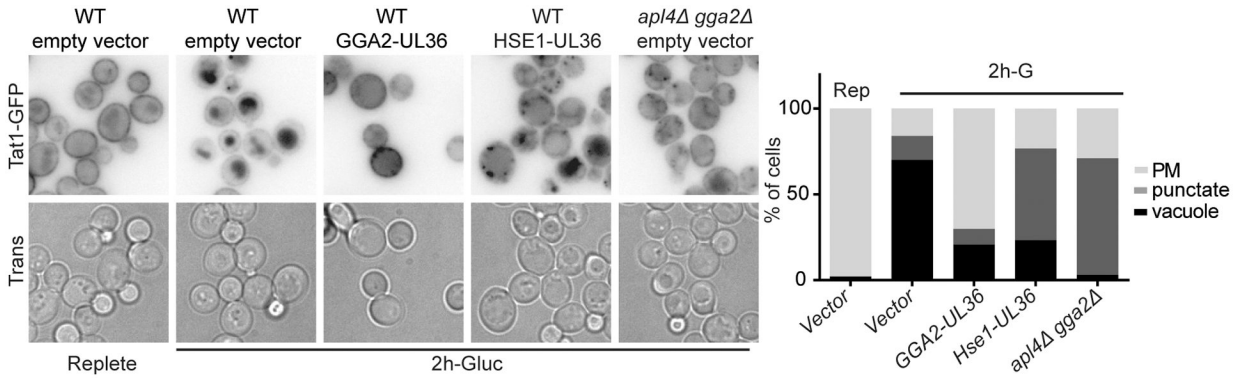

Figure 7.

Recycling machinery is functional during glucose starvation. Cells expressing Tat1-GFP from its endogenous locus and indicated UL36 fusions or empty vector were imaged 2 hrs after glucose starvation. Charts show percent of cells of indicated class.

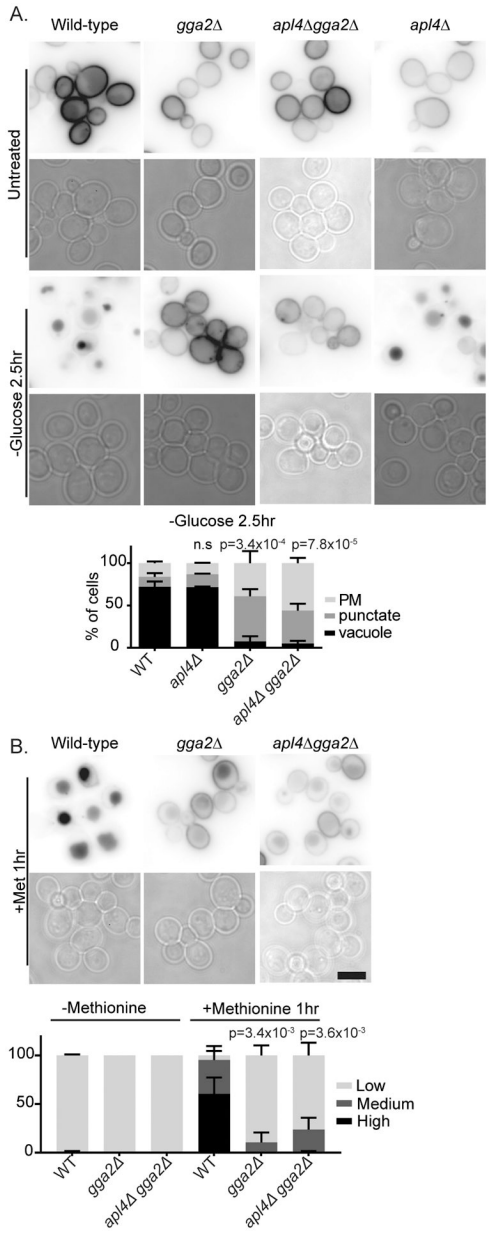

Figure 8.

Deletion of *GGA2* impairs vacuolar protein sorting. Indicated cells expressing Mup1-GFP from a plasmid were imaged under normal growth conditions (untreated), or after 2.5 hrs of glucose starvation or 1 hr of treatment with Methionine. For glucose starvation, chart shows quantification of cell classes as described in materials and methods, means with standard deviation are displayed, p=values were calculated using a two-tailed unpaired t-test for the null hypothesis that the percentage of cells with vacuolar localization was equal for mutant and wild-type cells. For methionine treatment, chart shows cells classified by vacuole to plasma membrane ratio as described in materials and methods, p=values were calculated using a two-tailed unpaired t-test for the null hypothesis that the percentage of cells with

high vacuolar intensity was equal for mutant and wild-type cells, means with standard deviation are displayed, n=3.

Table 1

Yeast strains used

Strain	Description	Reference
BY4741	*MATa his3Δ0 leu2Δ0 ura3Δ0 met1Δ0*	Invitrogen
BY4742	*MATα his3Δ0 leu2Δ0 ura3Δ0 lys2Δ0*	Invitrogen
DLY003	*Mat a his3Δ1 leu2Δ0 ura3Δ0 lys2Δ0 ENT5-GFP(S65T)::His3MX*	Aoh et al. 2011
DLY004	*Mat a his3Δ1 leu2Δ0 ura3Δ0 lys2Δ0 GGA2-GFP(S65T)::KanMX6*	Aoh et al. 2011
DLY 036	*MAT a his3Δ0 leu2Δ0 ura3Δ0 met1Δ0 APL4-GFP(S65T)::KanMX6*	Aoh et al. 2011
DLY037	*MATa his3Δ0 leu2Δ0 ura3Δ0 met1Δ0 ENT5-GFP(S65T)::KanMX6 SEC7-mCherry::His3MX*	This Study
DLY605	*MATa his3Δ0 leu2Δ0 ura3Δ0 met1Δ0 TAT1-GFP::KanMX6*	Invitrogen
DLY644	*MATα his3Δ0 leu2Δ0 ura3Δ0 ent3Δ::KanMX6 ent5Δ::KanMX6*	This Study
DLY646	*MATα his3Δ0 leu2Δ0 ura3Δ0 met1Δ0 ent5Δ::KanMX6 gga2Δ::KanMX6*	This Study
DLY650	*MATα his3Δ0 leu2Δ0 ura3Δ0 lys2Δ0 apl4Δ::KanMX6 gga2Δ::KanMX6*	This Study
DLY651	*MATa his3Δ0 leu2Δ0 ura3Δ0 apl4Δ::KanMX6 gga2Δ::KanMX6*	This Study
DLY656	*MATa his3Δ0 leu2Δ0 ura3Δ0 met1Δ0 apl4Δ::KanMX6 gga2Δ::KanMX6 TAT1-GFP::KanMX6*	This Study
DLY1183	*MATa his3Δ0 leu2Δ0 ura3Δ0 GGA2-mCherry::KanMX6*	This Study
DLY1920	*MATα his3Δ0 leu2Δ0 ura3Δ0 met1Δ0 gga2Δ::KanMX6*	This Study
DLY1954	*MATa his3Δ0 leu2Δ0 ura3Δ0 apl4Δ::KanMX6*	This Study
DLY2020	*MATa his3Δ0 leu2Δ0 ura3Δ0*	This Study
DLY2021	*MATα his3Δ0 leu2Δ0 ura3Δ0*	This Study
DLY2199	*MATα his3Δ0 leu2Δ0 ura3Δ0 lys2Δ0 CAN1-GFP::His3MX ENT5-mCherry::His3MX*	This Study
DLY2500	*MATa his3Δ0 leu2Δ0 ura3Δ0 Can1–3HA::His3MX*	This Study
DLY2548	*MATα his3Δ0 leu2Δ0 ura3Δ0 met1Δ0 ent3Δ::KanMX6 ent5Δ::KanMX6 CAN1–3HA::His3MX*	This Study
DLY2594	*MATα his3Δ0 leu2Δ0 ura3Δ0 met1Δ0 ent5Δ::KanMX6 gga2Δ::KanMX6 CAN1–3HA::His3MX*	This Study
DLY2595	*MATα his3Δ0 leu2Δ0 ura3Δ0 lys2Δ0 apl4Δ::KanMX6 gga2Δ::KanMX6 Can1–3HA::His3MX*	This Study
DLY2491	*his3Δ0/his3Δ0 leu2Δ0/leu2Δ0 ura3Δ0/ura3Δ0 MET15/MET15 LYS2/LYS2 SEC7-mCherry::His3MX/+*	This Study
QAY1239	*MATα his3Δ0 leu2Δ0 lys2Δ0 MET15+ ura3Δ0 erg6Δ::KanMX6 GGA2-mCherry::His3MX*	Aoh et al. 2013

Table 2

Plasmids used

Plasmid	Reference/ Source
pRS416-P_{Can1}-Can1-GFP	Lin et al., 2008
pRS416-P_{Mup1}-Mup1-GFP	Lin et al., 2008
pRS316-CUP1-TAT2-GFP-3XHA	Amy Chang
pRS316-Cup1-GGA2-UL36–3XHA	Stringer and Piper, 2011
pRS316-Cup1-Hse1-UL36–3XHA	Stringer and Piper, 2011
pRS316	Sikorskip and Heiter, 1989